Active Sites and Active Oxygen Species for Photocatalytic Epoxidation of Propene by Molecular Oxygen over TiO_2-SiO_2 Binary Oxides

Chizu Murata, Hisao Yoshida,* Jun Kumagai, and Tadashi Hattori

Department of Applied Chemistry, Graduate School of Engineering, Nagoya University, Nagoya 464-8603, Japan

Received: December 12, 2002; In Final Form: March 3, 2003

TiO_2-SiO_2 binary oxides of low Ti content promoted photocatalytic epoxidation of propene by molecular oxygen. By catalytic runs and UV spectra, it was revealed that the isolated tetrahedral Ti species on the TiO_2-SiO_2 samples are active for the photoepoxidation of propene, while the aggregated titanium oxide species are active mainly for the side reactions. By ESR and stoichiometric reaction tests of radical species, the following mechanism was proposed. Over the isolated tetrahedral Ti species, a $[Ti^{3+}-O_L^-]$* radical pair is formed by UV irradiation. The Ti^{3+} moiety reacts with O_2 to form O_2^-, which could not activate propene by itself. The O_L^- moiety, a hole center on lattice oxygen, reacts with O_2 to form O_3^-, and the O_3^- reacts with propene to yield PO. It is first suggested that the O_3^- is the electrophilic oxygen species effective for the epoxidation of propene. When the O_L^- moiety reacts with propene, acrolein or ethanal is produced through H abstraction or CC bond fission. The lower selectivity of the aggregated titanium oxide species was attributed to the lower stability of the O_3^- and high activity for the consecutive reaction of PO.

Introduction

Propene oxide (PO) is an intermediate for the chemical industry with a worldwide production capacity of nearly 5×10^6 tons per year.[1] Despite its importance, there is still no direct oxidation process by molecular oxygen for the preparation of PO.[1] Currently, industrial production of PO is performed by the chlorohydrin process or the hydroperoxide process. However, these processes suffer from byproducts and coproducts. Recently developed was propene epoxidation using H_2O_2 as oxidant with TS-1 catalyst.[2,3] This process is very selective to produce PO, and the only byproduct is H_2O, which is environmentally friendly. However, this process has not been commercialized widely because of the high cost of H_2O_2.

Many researchers have attempted the direct epoxidation of propene using molecular oxygen.[1] Although some workers have reported a new approach for propene epoxidation using O_2 and reducing agents such as H_2[4−6] and Zn powder,[7] it is certain that the process using only molecular oxygen and propene is the best for PO production. Several systems have been reported for the direct epoxidation of propene by using only molecular oxygen, for example, heterogeneous catalytic systems such as modified Ag catalysts,[1,8,9] metal nitrate-modified Ti-MCM catalysts,[10] zeolite-supported TiO_2 catalysts,[11] NaCl-modified $VCe_{1-x}Cu_x$ oxide catalysts,[12] and noncatalytic radical reaction systems.[13,14]

On the other hand, photosystems have been proposed as another potential approach for the epoxidation using only molecular oxygen.[15] The epoxidations of higher alkenes in the liquid phase using photocatalyst were reported in both heterogeneous[16−18] and homogeneous[19−21] systems. As for the photoepoxidation of propene, several systems using TiO_2,[22] Ba−Y type zeolite,[23−25] Nb_2O_5/SiO_2,[26] MgO/SiO_2, and SiO_2[27,28] have been reported. In the TiO_2 system, the selectivity to PO was low.[22] In other systems, the activity for photoepoxidation was still low and it was not clear whether the reaction proceeded catalytically.[23−28] In our previous screening study of silica-supported metal oxides for propene photoepoxidation, TiO_2/SiO_2 showed the highest PO yield.[29] In addition, we confirmed that the photoepoxidation of propene over TiO_2/SiO_2 proceeded catalytically, and the TiO_2-SiO_2 sample prepared by the sol−gel method showed higher PO selectivity than the sample prepared by the impregnation method.[30] In the present study we prepared a series of TiO_2-SiO_2 binary oxide samples containing different amounts of Ti to examine the active sites and the active oxygen species for propene photoepoxidation.

Experimental Section

TiO_2-SiO_2 binary oxide samples were prepared by the sol−gel method consisting of a two-stage hydrolysis procedure.[31] Tetraethoxyorthosilicate (Kishida), ethanol (Kishida), distilled water, and nitric acid (Kishida) were mixed in the amounts 0.5, 1.9, 0.5, and 0.043 mol, respectively. The mixture was stirred at 353 K for 3 h to hydrolyze tetraethoxyorthosilicate partially, and the obtained sol was cooled to room temperature. A 2-propanol (Kishida, 20 mL) solution of titanium isopropoxide (Kishida, 0.0005−0.05 mol) was added to the sol and stirred for 2 h. Then, an aqueous nitric acid solution (H_2O and HNO_3 were 0.5 and 0.043 mol, respectively) was added to the sol and stirred until the gelation was completed (about 3−14 days). The gel was heated to 338 K at the heating rate 0.2 K min^{-1} and dried for 5 h. After additional drying for 5 h at 373 K, it was calcined at 773 K in flowing air for 8 h. Ti content was determined by inductively coupled plasma (ICP) measurement. Titania−silica samples were denoted as T−S(x), where x (mol % of Ti) $= N_{Ti}/(N_{Ti} + N_{Si}) \times 100$. Amorphous silica was prepared from tetraethoxyorthosilicate by another sol−gel method followed by calcination in a flow of air at 773 K for 5 h.[29] The employed TiO_2 sample was a Japan Reference Catalyst (JRC-TIO-4; equivalent to P-25). The BET surface area of the samples was determined by N_2 adsorption after the sample was pretreated in a flow of He at 673 K for 0.5 h. The specific surface area of each TiO_2-SiO_2 and SiO_2 sample was similarly

10.1021/jp0277006 CCC: $25.00
Published on Web 04/11/2003

TABLE 1: Results of the Photooxidation of Propene over the SiO_2, TiO_2, and TiO_2-SiO_2 Samples[a]

						selectivity[c]/%						
run	sample	Ti content/mol %	surface area/$m^2\ g^{-1}$	conversion[b]/%	PO yield/%	PO	propanal	acetone	acrolein	ethanal	HC	CO_x
1	TiO_2-SiO_2	0.08	387	4.4	2.6	60.2	2.9	10.4	1.1	17.7	3.0	3.9
2		0.34	423	9.2	5.3	57.5	2.7	5.8	1.2	21.1	5.1	6.6
3		1.0	535	12.5	6.3	50.5	6.2	8.3	1.7	22.1	3.3	7.4
4		4.1	483	21.0	4.5	21.5	19.1	11.4	2.4	24.1	3.4	14.4
5		8.3	416	32.1	1.8	5.7	24.5	13.6	3.1	26.4	2.9	19.1
6[d]	TiO_2-SiO_2	0.34	423	0.2	trace	5.5	1.6	2.9	0.0	70.0	20.0	0.0
7[e]		0.34	423	0.9	trace	0.9	9.4	0.0	0.0	16.4	73.3	0.0
8	SiO_2		558	0.7	0.2	22.3	3.5	25.8	15.2	18.1	10.0	5.1
9[f]	TiO_2		34	14.1	0.0	0.0	0.0	1.3	0.0	0.8	1.7	96.2

[a] Catalyst 0.2 g, C_3H_6 100 μmol, O_2 200 μmol, reaction time 2 h. [b] Based on propene. [c] PO denotes propene oxide, HC denotes ethene + butenes, and CO_x denotes CO + CO_2. [d] In the dark at 330 K for 2 h. [e] In the absence of O_2. [f] Irradiation time was 1 h.

high enough (400−550 $m^2\ g^{-1}$), as shown in Table 1. Thus, in this study the conversion and PO yield were shown without normalization by surface area.

Prior to each reaction test and spectroscopic measurement, the sample was treated with 100 Torr oxygen (1 Torr = 133.3 N m^{-2}) at 773 K for 1 h, followed by evacuation at 673 K for 1 h. The photooxidation of propene was performed with a conventional closed system (123 cm^3). The sample (200 mg) was spread on the flat bottom (12.6 cm^2) of the quartz vessel. Propene (100 μmol, 15 Torr) and O_2 (200 μmol, 30 Torr) were introduced into the vessel, and the sample was irradiated by a 200 W Xe lamp. The temperature of the catalyst bed was elevated by ~20 K from room temperature due to the photoirradiation. After determination of the amount of CO and CO_2 in the gas phase by GC-TCD, the products and residual propene in the gas phase were collected by a liquid nitrogen trap and analyzed by GC-FID. After the nontrapped gas components (O_2 and CO) were evacuated, the catalyst bed was heated at 573 K in vacuo with a liquid nitrogen trap to collect the products desorbed from the catalyst. The results presented here are the sum of the product amounts collected at each step. Yield and selectivity were calculated on the basis of propene.

The reactivity of PO over the TiO_2-SiO_2 samples was tested in two ways: (A) Thermal reaction of PO; PO (20 μmol) was adsorbed by the sample in the dark at room temperature, and then the sample was heated at 573 K to collect the products by a liquid nitrogen trap. (B) Photooxidation of PO; PO (20 μmol) and O_2 (200 μmol) were introduced to the reactor, and then the sample was irradiated for 1 h. The products were collected and analyzed in the same manner as that for the reaction test of the propene photooxidation.

Temperature-programmed desorption of NH_3 (NH_3-TPD) was examined to estimate the amount of surface acid sites. The pretreated sample (300 mg) was exposed to NH_3 at 373 K for 0.5 h and evacuated at 373 K to remove weakly adsorbed NH_3 for 0.5 h. The temperature of the sample was linearly elevated to 1073 K by 5 K min^{-1} in a He carrier stream. The amount of desorbed NH_3 was monitored with the mass spectrometer at $m/e = 16$.

Diffuse reflectance UV spectra were recorded on a JASCO V-570 spectrophotometer at room temperature. ESR spectra were measured at 77 K by a X-band JEOL JES-TE200 spectrometer at a microwave power level (1.0 mW) at which microwave power-saturation of the signals did not occur. The sample was irradiated by a 500 W ultrahigh-pressure Hg lamp at 77 K. The magnetic field was calibrated with a JEOL NMR FIELD METER ES-FC5.

Results

Photooxidation of Propene by Molecular Oxygen over the TiO_2-SiO_2 Samples. Table 1 shows the results of photooxidation of propene over the TiO_2-SiO_2, SiO_2, and TiO_2 samples. Partial oxidation of propene took place over all the TiO_2-SiO_2 samples under the photoirradiation (runs 1−5). The major products were PO, ethanal, propanal, CO, CO_2, acetone, and acrolein; and small amounts of 2-propanol, ethene, and butene were also formed. It was confirmed that the epoxidation of propene did not proceed on the T−S(0.34) sample in the dark (run 6). In the absence of O_2, propene conversion was very low, and the main products were ethene, butane, and ethanal (run 7), which would be produced by the photometathesis of propene and the reaction between the lattice oxygen and propene.[28,32−37] This result indicates that molecular O_2 is essential for the photoepoxidation of propene over the TiO_2-SiO_2 samples. The SiO_2 sample showed low conversion and 22% PO selectivity (run 8),[29,30] while the TiO_2 sample showed high activity for the complete oxidation of propene to CO_2 (run 9),[30] as previously reported.

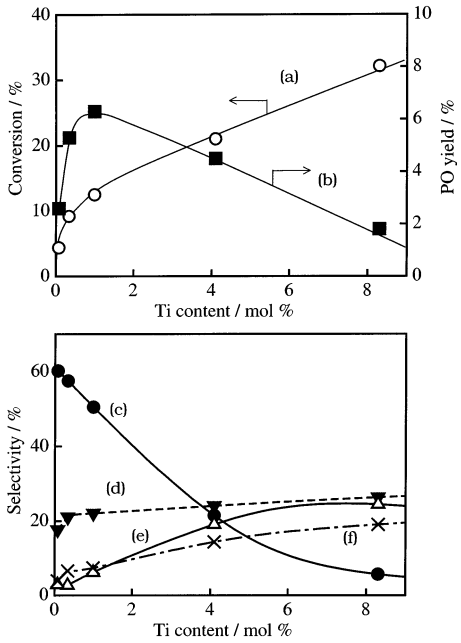

Figure 1. Results of the photooxidation of propene over TiO_2-SiO_2 samples. Conversion (a), PO yield (b), and selectivity to PO (c), ethanal (d), propanal (e), and CO + CO_2 (f).

Figure 1 depicts the results of photooxidation of propene over the TiO_2-SiO_2 samples from Table 1. The conversion of propene increased with an increase of Ti content, while the yield of PO increased with Ti content up to 1 mol % Ti and then decreased. The T−S(0.08) and T−S(0.34) samples showed high selectivity to PO, such as 60%. With increasing Ti content, the selectivity to PO decreased, while the selectivity to CO_2 and

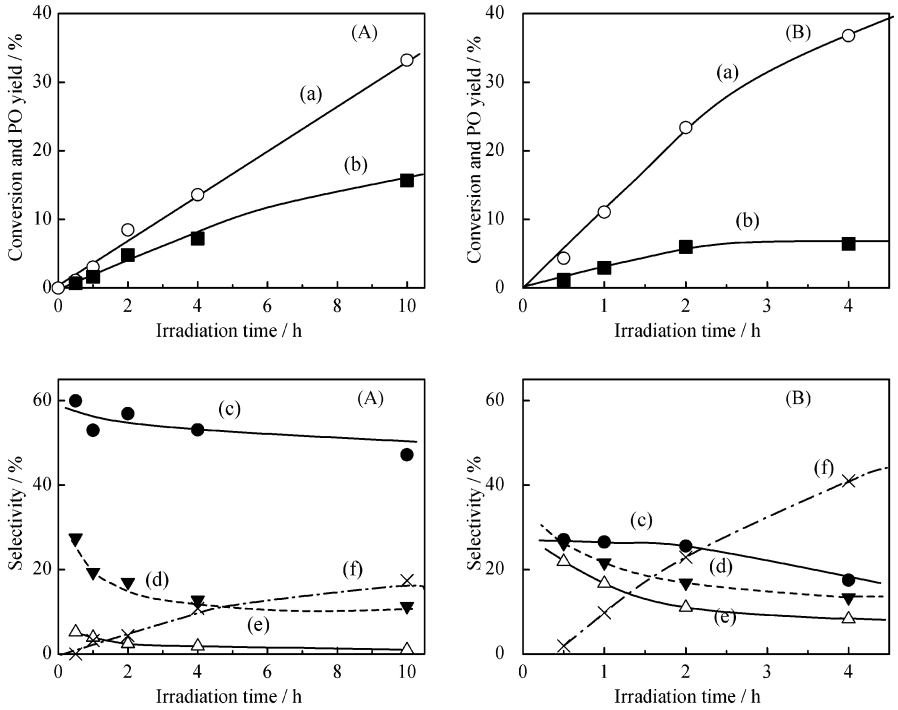

Figure 2. Time course of the photooxidation of propene over the T−S(0.34) (A) and T−S(4.1) (B) samples. Catalyst 0.2 g, C_3H_6 100 μmol, O_2 200 μmol. Conversion (a), PO yield (b), and selectivity to PO (c), ethanal (d), propanal (e), and CO + CO_2 (f).

propanal increased. Selectivity to ethanal was not so affected by Ti content.

Figure 2 shows time courses of propene photooxidation over the T−S(0.34) and T−S(4.1) samples. Over both samples, the conversion increased with an increase of irradiation time. With increasing conversion, the PO selectivity slightly decreased, and the selectivity to ethanal and propanal much decreased in the initial 2 h, while the selectivity to CO_x increased. This indicates that ethanal and propanal were consecutively oxidized to CO_x more easily than PO was. Comparing the selectivity at similar conversion, the difference between the T−S(0.34) and T−S(4.1) samples was evident. From the results in Figures 1 and 2, it was clearly shown that the TiO_2−SiO_2 samples with less Ti content are more effective for the photoepoxidation of propene. Over the T−S(0.34) sample the PO yield reached 15.7% at 10 h (Figure 2A). Even if all the Ti atoms were assumed to be the active sites, the turnover number, TON = (the amount of produced PO)/(the amount of active sites), was 1.4. This means that the photoepoxidation of propene over the TiO_2−SiO_2 samples proceeds catalytically in a similar manner as the previously reported result over the TiO_2−SiO_2 sample.[30]

Active Sites for Photoepoxidation of Propene on TiO_2−SiO_2 Samples. Diffuse reflectance UV spectroscopy was employed to determine the structure of Ti species on the TiO_2−SiO_2 samples (Figure 3). The TiO_2 sample showed a large absorption band below 400 nm. The SiO_2 sample scarcely showed absorption. The T−S(0.08) and T−S(0.34) samples exhibited a narrow absorption band below 250 nm centered at around 205 nm, which was assigned to the LMCT (ligand−metal charge transfer) from O to Ti (eq 1) of the isolated tetrahedral Ti species (isolated TiO_4 unit).[38−40]

$$[Ti^{4+}-O_L^{2-}] \overset{h\nu}{\rightleftharpoons} [Ti^{3+}-O_L^{-}]^* \qquad (1)$$

The samples containing more than 1 mol % Ti showed additional absorption bands above 250 nm, which are assigned to the

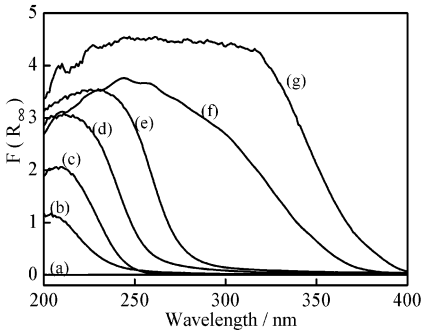

Figure 3. Diffuse reflectance UV spectra of SiO_2, TiO_2−SiO_2, and TiO_2 samples. SiO_2 (a), T−S(0.08) (b), T−S(0.34) (c), T−S(1.0) (d), T−S(4.1) (e), T−S(8.3) (f), and TiO_2 (g).

LMCT from O to Ti of aggregated titanium oxide species (aggregated TiO_x units, $x = 4-6$).[38−40] The absorption edge was shifted to longer wavelength with increasing Ti content and became close to that of the TiO_2 sample. It is generally known that the absorption edge is shifted to longer wavelength as the size of the aggregated species becomes larger and as the coordination number of Ti increases.[38−40] In the SiO_2-supported TiO_2 system, the following were suggested on the basis of UV−vis−NIR, Raman, and XANES spectroscopies: When the Ti content is low, the isolated TiO_4 units exist, and with increasing Ti content, one-dimensional polymerized TiO_4 units and two-dimensional polymerized TiO_5 units would be formed, followed by the formation of small particles comprised of TiO_6 units, and then the particle size becomes larger.[39] This spectroscopic aspect could be applied to the present TiO_2−SiO_2 binary oxide system; that is, the coordination number and the size of titanium oxide species should increase with increasing Ti content in the TiO_2−SiO_2 samples.

When compared with the results of reaction tests, it was demonstrated that the isolated tetrahedral Ti species on SiO_2 are responsible for propene photoepoxidation, while the ag-

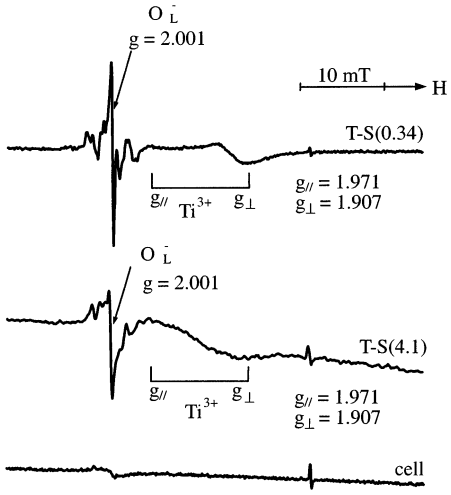

Figure 4. ESR spectra at 77 K of the T−S(0.34) and T−S(4.1) samples and cell after the photoirradiation in vacuo at 77 K.

gregated titanium oxide species are responsible for propanal, ethanal, and CO_x production.

Photoformed Radical Species on the TiO_2−SiO_2 Samples. The T−S(0.34) and T−S(4.1) samples showed no ESR signals in the dark at 77 K. UV irradiation of the T−S(0.34) and T−S(4.1) samples in vacuo at 77 K gave rise to the ESR signals shown in Figure 4. Both samples showed ESR signals with an axial symmetric g tensor assigned to Ti^{3+} ($g_{||} = 1.971$ and $g_{\perp} = 1.907$),[41−46] and a signal due to O_L^- ($g = 2.001$), a hole center on the lattice oxygen.[46,47] This hole center has also been observed over some irradiated systems, for example, UV-irradiated TiO_2[41−45] and γ-irradiated silica-based materials.[46,47] It was verified that UV irradiation results in the LMCT from O to Ti (eq 1). The signals attributed to Ti^{3+} and O_L^- were stable at 77 K after the photoirradiation was stopped. When the sample was warmed to room temperature, these signals disappeared.

When the T−S(0.34) sample was irradiated at 77 K in the presence of O_2 (1.0 Torr), the signals shown in Figure 5a (solid line) were observed. In the range from 0.1 to 30 Torr O_2, the intensity and shape of ESR spectra were analogous to each other for the T−S(0.34) sample. The heights of these signals were about 10 times larger than those of Ti^{3+} and O_L^-. Without UV irradiation, no signals appeared. These photoformed signals were stable at 77 K even after the photoirradiation was turned off. The total spectrum was attributed to the superimposition of the O_2^- ($g_{xx} = 2.003$, $g_{yy} = 2.009$, $g_{zz} = 2.025$)[48−50] and T-type O_3^- ($g_{||} = 2.008$, $g_{\perp} = 2.002$)[49−51] signals. The shape of T-type O_3^- is shown in the following model:

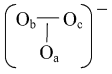

When the sample was warmed to room temperature for several minutes, the O_3^- signal disappeared and only the O_2^- signal remained (Figure 5b (broken line)). This O_2^- is very stable, and the intensity of the O_2^- signal very slowly decreased at room temperature in several days while the O_3^- on the TiO_2−SiO_2 samples was unstable at room temperature.

These oxygen radicals are also observed over the T−S(4.1) sample, similarly to the case of the T−S(0.34) sample (Figure 5). However, the ratio of the two radicals was obviously different. The relative amount of O_3^- and O_2^- was determined by the double integration of ESR signals. The ratios of O_3^-/O_2^- were 0.58 and 0.16 over the T−S(0.34) and T−S(4.1) samples, respectively. It was clearly shown that the O_3^- is more stable over the T−S(0.34) sample than over the T−S(4.1) sample.

It is known that O_2^- is generated by the reaction of Ti^{3+} with O_2 in the following equation:[48−51]

$$Ti^{3+} + O_2 \rightarrow Ti^{4+}-O_2^- \quad (2)$$

On the other hand, it is generally accepted that O_3^- is generated in the following scheme:[50]

$$O^- + O_2 \rightarrow O_3^- \quad (3)$$

In eq 3, two types of O^- have been proposed. One is generated by the dissociation of O_2^-.[52−54] Another is the hole trapping lattice oxygen, O_L^-.[51,55−57] In the present system, the O_L^- was generated by the photoirradiation in the absence of O_2 (Figure 4). In addition, both O_3^- and O_2^- were immediately generated by UV irradiation at 77 K, and the intensity of O_3^- and O_2^- signals increased with increasing irradiation time over both the T−S(0.34) and T−S(4.1) samples with constant ratio. These results suggest that O_3^- is formed by the reaction of O_L^- with O_2 in the following equation:

$$O_L^- + O_2 \rightarrow O_3^- \quad (4)$$

The introduction of propene into the samples containing O_2^- and O_3^- at 77 K in the dark did not change the O_2^- and O_3^- signals and produced no signals attributed to propene. The subsequent UV irradiation did not affect the signals. When the samples were warmed to room temperature, O_3^- disappeared and O_2^- remained even in the presence of propene. It is generally known that O_2^- is less reactive to hydrocarbon molecules than other oxygen species such as O^- and O_3^-.[50] These results suggest that the O_2^- is not active to propene by itself. On the other hand, since the O_3^- disappeared at room temperature in both the presence and absence of propene, the reactivity of the O_3^- to propene could not be confirmed by ESR, and it will be discussed later.

When the T−S(0.34) and T−S(4.1) samples were irradiated in the presence of propene (1.0 Torr) at 77 K without molecular oxygen, a complicated ESR signal was overlapped on the Ti^{3+} signal (Figure 6). The intensity of the Ti^{3+} signal in the presence of propene was larger than that in vacuo. In Figure 7, a sum of simulated spectra for $CH_2\dot{C}HCH_2$ (π-allyl radical, $g = 2.0023$, hyperfine coupling constant (hfcc), 0.406 mT for an α proton, 1.393 mT and 1.483 mT for two β protons, respectively),[58] $^{\bullet}CH_3$ (methyl radical, $g = 2.0023$, hfcc, 2.3 mT for three α protons),[58] and $H_3C(CH_2)_n\dot{C}HCH_3$ (alkyl radical, $g = 2.0023$, hfcc, 2.3 mT for three methyl β protons, 2.2 and 4.4 mT for methylene β protons of secondary radicals, the anisotropic hfcc values of the α proton were 1.17, 1.96, and 3.52 mT)[59] is compared with an experimental one. The simulated spectrum coincides with the experimental one very well except for the part of the Ti^{3+} signal at $g = 1.982$. From these results, it was suggested that O_L^- reacted with propene to form the allyl radical or methyl radical and that the consumption of the hole on O_L would stabilize Ti^{3+} as shown in eqs 5 and 6.

$$Ti^{3+}-O_L^- + H_2C{=}CH-CH_3 \rightarrow Ti^{3+}-O_LH + H_2C\dot{C}HCH_2 \quad (5)$$

$$Ti^{3+}-O_L^- + H_2C{=}CH-CH_3 \rightarrow Ti^{3+}-O_L-CH{=}CH_2 + {}^{\bullet}CH_3 \quad (6)$$

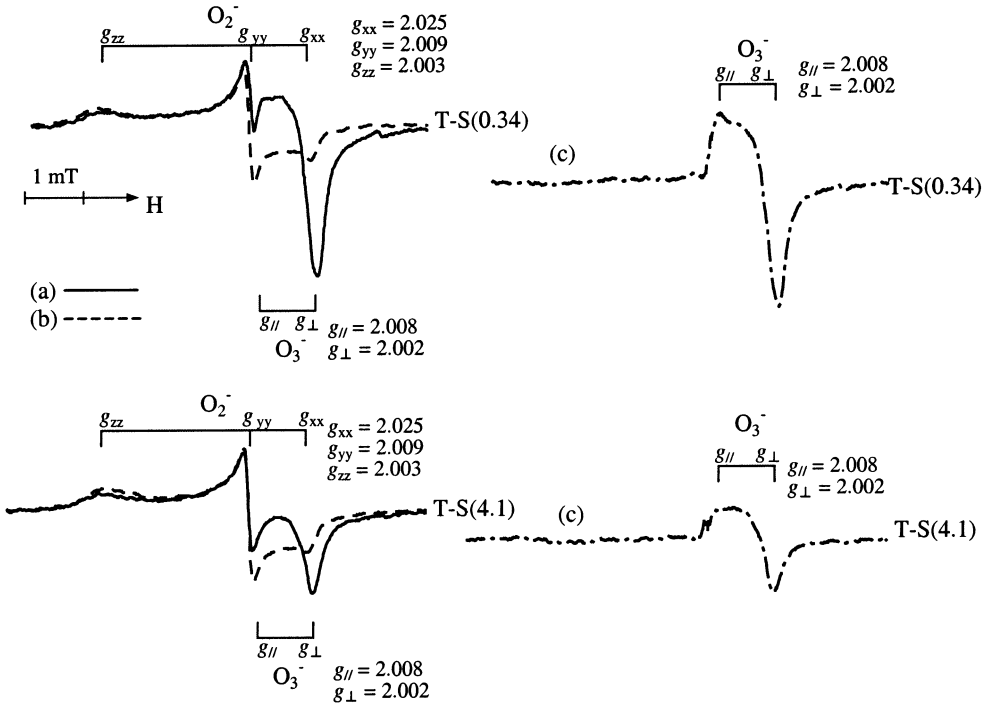

Figure 5. ESR spectra at 77 K of the T−S(0.34) and T−S(4.1) samples after the photoirradiation in the presence of O_2 (1.0 Torr) at 77 K (a), followed by warming the samples to room temperature for several minutes (b). The spectra in part c were obtained by subtracting spectra b from spectra a.

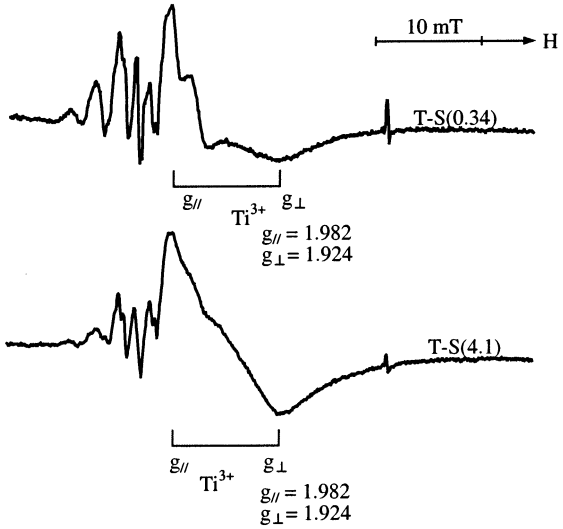

Figure 6. ESR spectra at 77 K of the T−S(0.34) and T−S(4.1) samples after the photoirradiation in the presence of propene (1 Torr) in the absence of O_2 at 77 K.

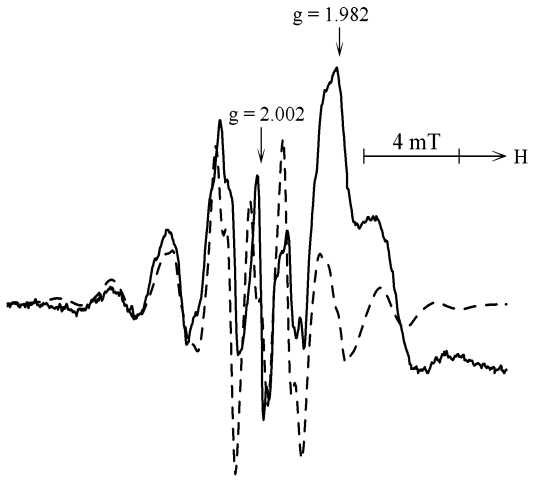

Figure 7. A sum of simulated ESR spectra (broken line) and observed ESR spectra (solid line) of the T−S(0.34) sample photoirradiated in the presence of propene (1.0 Torr) at 77 K. The following parameters are employed for the simulation. $CH_2\dot{C}HCH_2$ (π-allyl radical, g = 2.0023, hyperfine coupling constant (hfcc), 0.406 mT for an α proton, 1.393 mT and 1.483 mT for two β protons, respectively),[54] $^{\bullet}CH_3$ (methyl radical, g = 2.0023, hfcc, 2.3 mT for three α protons),[54] and H_3C-$(CH_2)_n\dot{C}HCH_3$ (alkyl radical, g = 2.0023, hfcc, 2.3 mT for three methyl β protons, 2.2 and 4.4 mT for methylene β protons of secondary radicals, the anisotropic hfcc values of the α proton were 1.17, 1.96, and 3.52 mT).[55] The relative ratio of $CH_2\dot{C}HCH_2$/$^{\bullet}CH_3$/$H_3C(CH_2)_n\dot{C}HCH_3$ is 1.0/0.1/4.4.

These allyl and methyl radicals would react with propene to produce the alkyl radical, $H_3C(CH_2)_n\dot{C}HCH_3$, in the following schemes:

$$H_2C{=}\dot{C}H{=}CH_2 + H_2C{=}CH{-}CH_3 \rightarrow H_2C{=}CH{-}CH_2{-}\dot{C}H{-}CH_3 \quad (7)$$

$$^{\bullet}CH_3 + H_2C{=}CH{-}CH_3 \rightarrow H_3C{-}CH_2{-}\dot{C}H{-}CH_3 \quad (8)$$

When O_2 (1 Torr) was subsequently added to the samples at 77 K, the Ti^{3+} signal decreased and the O_2^- signal appeared over both samples in addition to the signals derived from propene (Figure 8). This result indicates that the photoformed Ti^{3+} reacts with O_2 to produce O_2^- in the presence of O_2 and propene (eq 2), while the prodution of O_3^- (eq 4) does not occur after O_L^- reacts with propene. When these samples warmed to room temperature, the radical species derived from propene disappeared, and O_2^- remained. O_2^- was a stable species even in the presence of a propene molecule.

The Ti^{3+} signal of the T−S(0.34) sample almost disappeared by O_2 introduction, while that of the T−S(4.1) sample partly remained (Figure 8). This agrees well with the result that the T−S(4.1) sample contains the aggregated titanium oxide species (Figure 3). The T−S(0.34) sample would have Ti^{3+} species on

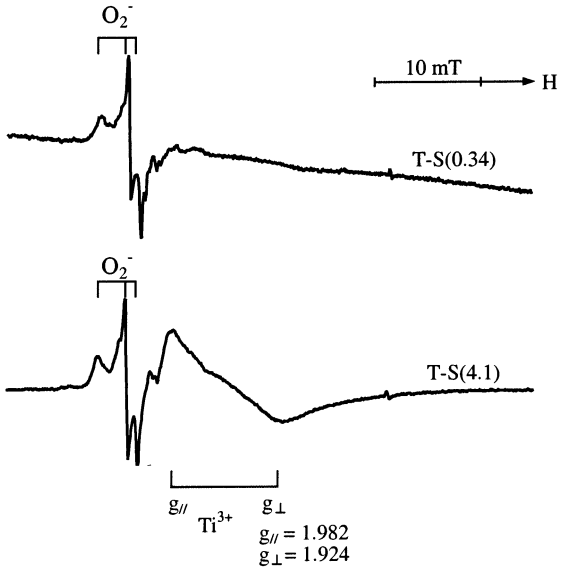

Figure 8. ESR spectra at 77 K of the T−S(0.34) and T−S(4.1) samples after the photoirradiation in the presence of propene (1.0 Torr) at 77 K, followed by the introduction of O_2 (1.0 Torr) in the dark at 77 K.

the surface predominantly, while the T−S(4.1) sample would have Ti^{3+} species not only on the surface but also in the bulk lattice in which the Ti^{3+} cannot contact with molecular oxygen.

Reactivity of the Oxygen Radical Species to Propene. ESR spectra showed that O_3^- and O_2^- were generated over the TiO_2−SiO_2 samples irradiated at 77 K in the presence of oxygen, while only O_2^- was observed at room temperature. On the other hand, it was confirmed that O_L^- reacted with propene to form allyl radical, methyl radical, and alkyl radical species by photoirradiation at 77 K. Therefore, it is expected that we can control the selective preparation of the oxygen radical species, O_3^-, O_2^-, and O_L^- and can examine their reactivity to propene. Since the amount of products collected by 573 K heating after ESR measurement was too small to be detected by GC-FID, we carried out separate experiments with larger amounts of samples (2.0 g) in the same procedures as ESR measurements in order to determine the products generated through the reaction of each oxygen species with propene.

Table 2 lists the procedures for obtaining each expected radical species and the products experimentally obtained by the stoichiometric reaction of radical species with propene or O_2. First, we will show the results over the T−S(0.34) sample, which contain the isolated tetrahedral Ti species predominantly. When propene and O_2 were introduced on the T−S(0.34) sample at 77 K in the dark and it was warmed to room temperature, no products were detected (method E, run 5). It was confirmed that the propene epoxidation does not proceed without UV irradiation.

In method A, O_2 was introduced into the T−S(0.34) sample, and the reactor was cooled to 77 K, followed by the photoirradiation at 77 K. This procedure should bring about O_3^- and O_2^- radical species on the T−S(0.34) sample according to eqs 1, 2, and 4. Subsequently, propene was introduced to the sample at 77 K and the sample was warmed to room temperature in the dark. By these procedures, it is expected that propene comes in contact with O_3^- and O_2^- on the T−S(0.34) sample. As a result, almost equimolecular amounts of PO and acetone were detected as products (run 1). In the actual reaction test (Table 1), the selectivity to acetone was less than 10%. The quite different reaction conditions, such as temperature and products' yield, between these experiments would result in the discrepancy of acetone selectivity.

In method B, propene was introduced into the T−S(0.34) sample, and the reactor was photoirradiated at 77 K, followed by O_2 introduction at 77 K in the dark. This procedure will bring about allyl radial, methyl radical, alkyl radical, and O_2^- radical species on the T−S(0.34) sample according to eqs 1, 2, and 5−8. After the sample was warmed to room temperature, ethanal, acrolein, and propanal were mainly obtained (run 2).

In method C, after the T−S(0.34) sample was photoirradiated at 77 K in the presence of O_2 and warmed to room temperature, only the O_2^- species was confirmed by the separate ESR measurement (eqs 1 and 2). When propene was introduced to this sample, ethanal, propanal, and acrolein were mainly generated (run 3). This product distribution is very similar to that by method B (run 2).

In method D, the T−S(0.34) sample was reduced by H_2 at 773 K and evacuated at 773 K, followed by O_2 introduction at room temperature. This reduction procedure generates Ti^{3+} on the sample in the following scheme:[48,50]

$$Ti^{4+} \xrightarrow{H_2\ \text{reduction}} Ti^{3+} \qquad (9)$$

The Ti^{3+} immediately reacts with O_2 to produce O_2^- according to eq 2.[48,50] The existence of O_2^- was confirmed by ESR. When this O_2^- species was contacted with propene at room temperature, no products were detected (run 4). This confirmed that the O_2^- on the TiO_2−SiO_2 samples is not active to propene at room temperature, as described above.

From the results of runs 1 and 4 in Table 2 (methods A and D), it was revealed that O_3^- reacts with propene to produce PO; in other words, O_3^- is the active oxygen species for the photoepoxidation of propene over the isolated tetrahedral Ti species. On the other hand, the result of run 3 in Table 2 (method B) demonstrated that the O_L^- reacts with propene to produce ethanal and acrolein.

Runs 6−8 in Table 2 show the results over the T−S(4.1) sample, which also contains the aggregated titanium oxide species. In methods A−C, PO was not generated at all, while ethanal, acrolein, and propanal were mainly obtained (runs 6−8). This product distribution is quite different from that of the actual reaction test (Table 1). Details will be discussed below.

Consecutive Reaction of Propene Oxide over the TiO_2−SiO_2 Samples. To know the possibility of the consecutive conversion of produced PO, the thermal reaction and the photooxidation of PO were examined over the T−S(0.34) and T−S(4.1) samples (Table 3). By the thermal reaction, PO was isomerized mainly to propanal. The amount of converted PO over the T−S(0.34) sample (run 1) was very small in comparison with that over the T−S(4.1) sample (run 2).

It is generally known that PO is isomerized into propanal on acid sites and into acetone on basic sites.[60] The amount of surface acid sites was estimated from NH_3-TPD and shown in Table 3. The T−S(0.34) sample showed a very small amount of acid sites (3 μmol g^{-1}), which is a comparable level to that of the SiO_2 sample (<6 μmol g^{-1}). The T−S(4.1) sample was found to have 55 μmol g^{-1} of acid sites. This means that the Ti species on the T−S(0.34) sample do not act as acid sites, while those on the T−S(4.1) sample result in acid sites. It is generally considered that Ti−O−Si bridges adjacent to TiO_5 units and TiO_6 units cause the charge imbalance to exhibit acidity, while TiO_4 units bring about no acid sites.[38] This agrees well with the results mentioned above. The acid sites derived from the aggregated titanium oxide species on the T−S(4.1) sample would convert PO into propanal through the thermal reaction.

The photooxidation of PO with molecular oxygen followed by thermal desorption was also examined. Ethanal and CO_x were

TABLE 2: Results of Stoichiometric Reaction of Oxygen Radical Species with Propene[a]

run	sample	method[b]	expected radical species[c]	products[d]/%
1	T−S(0.34)	A	O_3^-, O_2^-	PO (52), acetone (48)
2		B	O_2^-, methyl radical, allyl radical, alkyl radical	ethanal (49), acrolein (24), propanal (15), PO (4), acetone (8)
3		C	(O_L^-),[e] O_2^-	ethanal (49), acrolein (25), propanal (19), PO (3), acetone (4)
4[f]		D	O_2^-	none
5		E	none	none
6	T−S(4.1)	A	O_3^-, O_2^-	ethanal (52), acrolein (33), propanal (15)
7		B	O_2^-, methyl radical, allyl radical, alkyl radical	ethanal (52), acrolein (9), propanal (8), acetone (20), C_2H_4 (11)
8		C	(O_L^-),[e] O_2^-	ethanal (53), acrolein (33), propanal (14)

[a] Catalyst 2 g, O_2 5 μmol, C_3H_6 20 μmol, irradiation time 0.5 h. [b] The methods are composed of the following sequential procedures. [A] (1) The sample was irradiated at 77 K in the presence of O_2. (2) C_3H_6 was introduced to the sample at 77 K in the dark. (3) The sample was warmed to room temperature in the dark. [B] (1) The sample was irradiated at 77 K in the presence of C_3H_6. (2) O_2 was introduced to the sample at 77 K in the dark. (3) The sample was warmed to room temperature in the dark. [C] (1) The sample was irradiated at 77 K in the presence of O_2. (2) The sample was warmed to room temperature in the dark. (3) C_3H_6 was introduced to the sample at room temperature in the dark. [D] (1) The sample was reduced by H_2 at 723 K for 1 h. (2) The sample was evacuated at 723 K for 1 h. (3) O_2 was introduced to the sample at room temperature in the dark. (4) C_3H_6 was introduced to the sample at room temperature in the dark. [E] (1) O_2 and C_3H_6 were introduced to the sample at 77 K in the dark. (2) The sample was warmed to room temperature in the dark. [c] The expected radical species. The existence of a radical species was confirmed by separate ESR measurements. [d] The products were collected by heating at 573 K in vacuo with a liquid nitrogen trap after the procedures shown in methods A−E. The percentage of each product is shown in parentheses. [e] It could not be confirmed by separate ESR measurement. [f] Catalyst 10 g.

TABLE 3: Results of the Reaction of Propene Oxide over the TiO_2−SiO_2 Samples[a]

				collected compounds/μmol							
run	sample	Ti atoms[b]/(μmol g^{-1})	acid sites[c]/(μmol g^{-1})	propanal	acetone	acrolein	ethanal	alcohols	HC	CO_x[d]	sum/μmol
				thermal reaction[e]							
1	T−S(0.34)	55	3	0.3	trace	trace	trace	0.0	trace	trace	0.4
2	T−S(4.1)	675	55	2.9	0.1	0.0	trace	0.0	0.2	0.6	3.8
				photooxidation[f]							
3	T−S(0.34)	55	3	0.3	0.1	0.0	0.3	0.0	trace	0.3	1.0
4	T−S(4.1)	675	55	3.7	0.5	0.5	1.2	0.7	0.3	1.0	7.9

[a] Catalyst 0.2 g. [b] The number of Ti atoms contained in 1 g of the sample. [c] The amount of acid sites calculated from the NH_3−TPD profile. [d] CO_x denotes CO + CO_2. [e] The thermal reaction of propene oxide (20 μmol) by 573 K heating in vacuo. [f] The photooxidation of propene oxide (20 μmol) for 1 h with O_2 (200 μmol), followed by the thermal desorption of products by heating at 573 K.

mainly obtained in addition to propanal over both samples (runs 3 and 4). In the photooxidation, the T−S(4.1) sample converted more PO than the T−S(0.34) sample did. This agrees with the high activity for complete photooxidation of the bulk TiO_2 sample (Table 1, run 9). It is demonstrated that the aggregated titanium oxide species promotes not only the thermal isomerization of PO to propanal on the acid sites but also the consecutive photooxidation of PO to CO_x.

Discussion

Proposed Mechanism for the Photooxidation of Propene over the Isolated Tetrahedral Ti Species. As described above, the O_3^- reacts with propene to produce PO. Kanai et al. reported TiO_2−SiO_2 containing 5 mol % Ti produced PO in the photooxidation of propene although the selectivity to PO was low.[61] Without direct experimental evidence, they speculated that PO was produced through a titanaoxacyclobutane intermediate that was produced by the reaction of propene with O_L^-. From the results in the present study, the reaction between propene and O_L^- provided other products. Therefore, their speculation seems to be excluded.

The O_L^- reacted with propene to produce methyl radical and allyl radical. When the radical species contacted with molecular oxygen, ethanal, acrolein, and propanal were mainly obtained (method B, run 2). Yoshida et al. suggested that the photoexcited V═O bonds on V_2O_5/SiO_2 catalyst (5 wt % V_2O_5) activate propene and O_2 to produce a π-allyl intermediate and O_2^-, and then ethanal or acrolein is generated.[62] Xiang et al. speculated that propene cation radical $C_3H_6^+$ and O_2^- are generated through an intermolecular C_3H_6−O_2 charge transfer in the cage of Ba-exchange zeolites and lead to ethanal and formaldehyde or acrolein and H_2O.[25] In the present study, the reaction of O_L^- with propene resulted in methyl radical or allyl radical through CC bond fission or H abstraction (Figure 6). These radical species would react with O_2^- to form ethanal and formaldehyde or acrolein and H_2O. However, as described in the previous section, the O_2^- remained after the hydrocarbon radical species disappeared at room temperature. The possibility of direct reaction with molecular oxygen could not be excluded.

The products distribution obtained in method C was very similar to that obtained in method B. This result implied that O_L^- also existed on the samples at room temperature after the photoirradiation at 77 K in the presence of O_2 although the signal of O_L^- was not observed by ESR measurement (Figure 5b). The O_L^- would be formed through the decomposition of O_3^- at room temperature (the reverse reaction of eq 4). The spin−lattice relaxation time of the O_L^- might become shorter because the symmetry is changed by the presence of the O_2^-.

From these results, the tentative mechanism for the photooxidation of propene at room temperature over the isolated tetrahedral Ti species is proposed in Scheme 1. When the [Ti^{4+}−O_L^{2-}] of the isolated tetrahedral Ti species (species I) absorbs UV light (λ < 250 nm), LMCT from O to Ti occurs, and the charge-transfer exited state [Ti^{3+}−O_L^-]* is achieved (species II). When the photoformed Ti^{3+} and O_L^- react with O_2, O_2^- and O_3^- are produced, respectively (species III). The O_3^- reacts with propene (species IV) to produce PO (route A); otherwise, it decomposes to O_L^- and O_2 (species V).

It is not clear how the O_2^- and the residual oxygen atom in O_3^- are consumed in route A after producing PO. However, since the selectivity to PO over the TiO_2−SiO_2 samples in the reaction test reached 60%, the residual oxygen atom in O_3^-

SCHEME 1: Proposed Mechanism for the Formation of PO, Ethanal, and Acrolein over the Isolated Tetrahedral Ti Species[a]

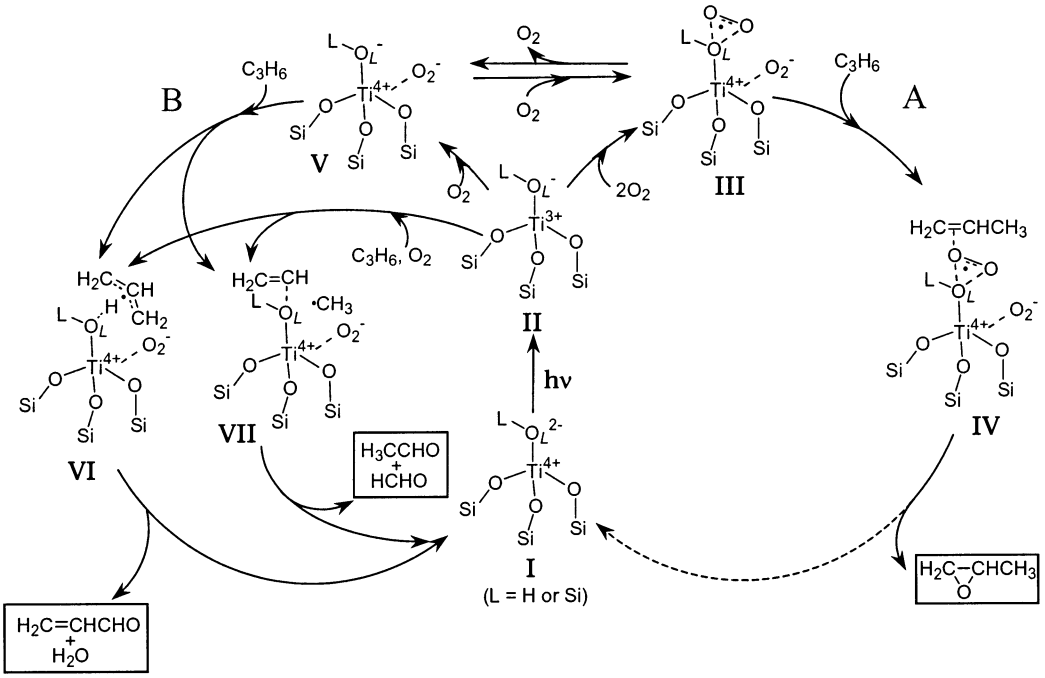

[a] Route A is the cycle for PO production through species I−II−III−IV−I. Route B is the cycle for acrolein or ethanal production through species I−II−(V)−VI or VII−I. L denotes either H or Si.

should not be responsible for side reactions and might produce one more PO. If two oxygen atoms in O_3^- are employed for the PO production, TON (produced PO/Ti atoms) should exceed 2 per one catalytic cycle. Although confirmed TON was 1.4 over the T−S(0.34) sample in the present study, confirmed TON reached 2.8 over the TiO_2/SiO_2 0.1 mol % sample, as previously reported.[30] This indicates that route A in Scheme 1 proceeds catalytically in any case.

When O_L^- reacts with propene, allyl radical (species VI) or methyl radical (species VII) is formed through H abstraction or CC bond fission. These radical species reacted with O_2^- or O_2 to produce acrolein and H_2O or ethanal and formaldehyde (route B). O_2 and propene would competitively react with the O_L^- to form the O_3^- and the hydrocarbon radical species, respectively, resulting in the different products from each other.

It is not clear whether both O_3^- and O_2^- coexist on the same [Ti−O] site (species III). However, since no Ti^{3+} signal was observed in the presence of O_2 under the photoirradiation, it may be more possible that the O_3^- and O_2^- coexist on the same [Ti−O] site. The existence of O_2^- on Ti^{3+} might result in the separation of electric charge to stabilize the existence of O_3^-. Thus, we tentatively draw O_3^- and O_2^- on the same [Ti−O] site in Scheme 1.

Electrophilic Active Oxygen Species for the Photoepoxidation of Propene. It is generally considered that the electrophilic oxygen species are effective for the epoxidation of alkene.[63−67] In the Ag/Al_2O_3 catalytic system for epoxidation of ethylene using molecular oxygen, it is suggested that the electrophilic atomic oxygen on the Ag surface attacks the C=C bonds in ethylene.[65] In the epoxidation system using peroxide reagents in the presence of homogeneous (Mo, W, V, Ti, and Zr) or heterogeneous (TiO_2/SiO_2, TS-1) catalysts, the peroxo species, generated from metal species and peroxide reagent, are suggested to be the active oxygen species.[66,67] It is considered that the metal ion increases the electrophilicity of the peroxo moiety by withdrawing electrons. It is well-known that cytochrome P-450, a monooxygenase, generates the electrophilic oxygen species from O_2 involving a reducing agent to catalyze the epoxidation of alkenes and hydroxylation of alkanes and aromatics.[68] Recently, many workers examined the epoxidation of olefin in the presence of O_2 and reducing agents in order to produce the electrophilic oxygen species.[4−7,63,64]

In the present study, O_3^- is claimed to be the active oxygen species for the epoxidation of propene. The O_3^- is generated by the reaction of the photoformed O_L^- (hole center on lattice oxygen) with O_2. Therefore, the O_3^- should be the electron deficient state and should have an electrophilic nature. So far, O_3^- was observed over various photoirradiated metal oxides and was suggested to be the active oxygen species for the $^{16}O-^{18}O$ exchange reaction and CO oxidation.[50,55,56,69−71] However, there are no reports that O_3^- on metal oxide reacts with alkene to produce epoxide. Takita et al. reported that the stoichiometric reaction between propene and O_3^- on MgO gave CO_2 as a main product.[72] The shape of the O_3^- on MgO is shown in the following model:

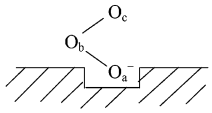

This is different from that on the TiO_2-SiO_2 samples. Therefore, the nature of the O_3^- would also be different. Kubokawa et al. reported that O_3^- was the active oxygen species for the photooxidation of alkenes to ketones, aldehydes, and dienes over porous Vycor glass (PVG).[73] The O_3^- on PVG is T-type O_3^-, similar to that on the TiO_2-SiO_2 samples; however, the reactivity to alkene is different. Since it is known that the nature of O^- strongly depends on the adjacent metal atoms,[50] that of O_3^- is also expected to vary from oxide to oxide. Other factors than the oxygen species would also be concerned. PVG is a porous silica material containing some impurities such as B_2O_3 (2.95 wt %), Na_2O (0.04 wt %), Al_2O_3, and ZrO_2 (0.72 wt %),

and it is expected to have acid sites. In our previous study, the Al_2O_3/SiO_2 sample showed low selectivity to PO because of its acidity.[29] The acidity on PVG might cause the absence of epoxide yield. The existence of T-type O_3^- would be required for the photoepoxidation; however, the other factor, such as acidity, will also be concerned with the photoepoxidation activity.

Effect of the Structure of Ti Species on the Photoepoxidation Activity. As shown in Table 1, the T−S(4.1) sample showed lower selectivity to PO (21.5%) than the T−S(0.34) sample (57.5%). The lower selectivity over the T−S(4.1) sample related to a lower ratio of O_3^-/O_2^- (Figure 5), which should correspond to species III/(species III + species V) in Scheme 1. Thus, route B is mainly promoted, or route A is less promoted over the aggregated titanium oxide species because of the smaller amount of O_3^-.

In the stoichiometric reactions over the T−S(4.1) sample, when propene was contacted with O_3^- and O_2^-, PO was not obtained, but ethanal, acrolein, and propanal were formed (Table 2, run 6). The products distribution is essentially identical to that obtained in method C (run 8). The O_3^- over the T−S(4.1) sample in method A (run 6) would decompose to O_L^- and O_2 before it reacts with propene during warming the sample from 77 K to room temperature. This result indicates that the O_3^- over the aggregated titanium oxide species would be unstable and more likely to decompose to O_L^- and O_2 than that over the isolated tetrahedral Ti species. This difference in stability of the O_3^- would be the major reason the isolated tetrahedral Ti species is effective for PO production.

In addition, the consecutive reaction of PO is little promoted over the isolated tetrahedral Ti species, while it is promoted over the aggregated titanium oxide species (Table 3). This would also cause the difference of the selectivities of these species.

Conclusion

The isolated tetrahedral Ti species on the TiO_2-SiO_2 samples catalyze the photoepoxidation of propene with molecular oxygen. $[Ti^{4+}-O_L^{2-}]$ is excited by UV light to form a $[Ti^{3+}-O_L^-]$* radical pair. The Ti^{3+} moiety reacts with O_2 to form O_2^-. The O_L^- moiety, a hole center on lattice oxygen, reacts with O_2 to form O_3^-, which reacts with propene to yield PO. The O_3^- would be the electrophilic oxygen species effective for the epoxidation of propene. When the O_L^- moiety reacts with propene, acrolein or ethanal is produced through H abstraction or CC bond fission.

The isolated tetrahedral Ti species exhibit the higher stability of the O_3^- and lower activity for the consecutive reactions of PO in comparison with the case of the aggregated titanium oxide species. This would explain the effectiveness of the isolated tetrahedral Ti species for PO production.

Acknowledgment. We thank Prof. Y. Okamoto, Dr. Y. Isobe (Department of Applied Chemistry, Graduate School of Engineering, Nagoya University), Mr. Y. Nagara, and Mr. M. Kawahara (Japan Chemical Innovation Institute, Nagoya) for their aid in ESR measurement. This work was supported by a grant-in-aid from the Japanese Ministry of Education, Science, Art, Sports and Culture, and by Nippon Sheet Glass Foundation for Materials Science and Engineering.

References and Notes

(1) Monnier, J. R. *Appl. Catal. A* **2001**, *221*, 73 and references therein.
(2) Clerici, M. G.; Bellussi, G.; Romano, U. *J. Catal.* **1991**, *129*, 159.
(3) Notari, B. *Adv. Catal.* **1996**, *41*, 253.
(4) Hayashi, T.; Tanaka, K.; Haruta, M. *J. Catal.* **1998**, *178*, 566.
(5) Haruta, M.; Daté, M. *Appl. Catal. A* **2001**, *222*, 427 and references therein.
(6) Meiers, R.; Dingerdissen, U.; Hölderich, W. F. *J. Catal.* **1998**, *176*, 376.
(7) Yamanaka, I.; Nakagaki, K.; Otuka, K. *J. Chem. Soc., Chem. Commun.* **1995**, 1185.
(8) Lu, G.; Zuo, X. *Catal. Lett.* **1999**, *58*, 67.
(9) Lu, J.; Luo, M.; Lei, H.; Li, C. *Appl. Catal. A* **2002**, *237*, 11.
(10) Miyaji, T.; Wu, P.; Tatsumi, T. *Catal. Today* **2001**, *71*, 169.
(11) Murata, K.; Kiyozumi, Y. *Chem. Commun.* **2001**, 1356.
(12) Lu, J.; Luo, M.; Lei, H.; Bao, X.; Li, C. *J. Catal.* **2002**, *211*, 552.
(13) Hayashi, T.; Han, L. B.; Tsubota, S.; Haruta, M. *Ind. Eng. Chem. Res.* **1995**, *34*, 2298.
(14) Nijhuis, T. A.; Musch, S.; Makkee, M.; Moulijn, J. A. *Appl. Catal. A* **2000**, *196*, 217.
(15) Maldotti, A.; Molinari, A.; Amadelli, R. *Chem. Rev.* **2002**, *102*, 3811.
(16) Kanno, Y.; Oguchi, T.; Sakuragi, H.; Tokumaru, K. *Tetrahedron Lett.* **1980**, *21*, 467.
(17) Fox, M. A.; Chen, C. *J. Am. Chem. Soc.* **1981**, *103*, 6757.
(18) Ohno, T.; Nakabeya, K.; Matsumura, M. *J. Catal.* **1995**, *176*, 76.
(19) Matsuda, Y.; Sakamoto, S.; Koshima, H.; Murakami, Y. *J. Am. Chem. Soc.* **1985**, *107*, 6415.
(20) Weber, L.; Imiolczyk, I.; Haufe, G.; Rehorek, D.; Hennig, H. *J. Chem. Soc., Chem. Commun.* **1991**, 301.
(21) Weber, L.; Hommel, R.; Behling, J.; Haufe, G.; Hennig, H. *J. Am. Chem. Soc.* **1994**, *116*, 2400.
(22) Pichat, P.; Herrmann, J.; Disdier, J.; Mozzanega, M. *J. Phys. Chem.* **1979**, *83*, 3122.
(23) Blatter, F.; Sun, H.; Frei, H. *Catal. Lett.* **1995**, *35*, 1.
(24) Blatter, F.; Sun, H.; Vasenkov, S.; Frei, H. *Catal. Today* **1998**, *41*, 297.
(25) Xiang, Y.; Larsen, S. C.; Grassian, V. H. *J. Am. Chem. Soc.* **1999**, *121*, 5063.
(26) Tanaka, T.; Nojima, H.; Yoshida, H.; Nakagawa, H.; Funabiki, T.; Yoshida, S. *Catal. Today* **1993**, *16*, 297.
(27) Yoshida, H.; Tanaka, T.; Yamamoto, M.; Funabiki, T.; Yoshida, S. *Chem. Commun.* **1996**, 2125.
(28) Yoshida, H.; Tanaka, T.; Yamamoto, M.; Yoshida, T.; Funabiki, T.; Yoshida, S. *J. Catal.* **1997**, *171*, 351.
(29) Yoshida, H.; Murata, C.; Hattori, T. *J. Catal.* **2000**, *194*, 364.
(30) Yoshida, H.; Murata, C.; Hattori, T. *Chem. Commun.* **1999**, 1551.
(31) Lange, R.; Hekkink, J.; Keizer, K.; Burggraaf, A. *J. Noncryst. Solids* **1995**, *191*, 1.
(32) Anpo, M.; Tanahashi, I.; Kubokawa, Y. *J. Chem. Soc., Faraday Trans.* **1982**, *78*, 2121.
(33) Anpo, M.; Kondo, M.; Kubokawa, Y.; Louis, C.; Che, M. *J. Chem. Soc., Faraday Trans.* **1988**, *84*, 2771.
(34) Yoshida, H.; Tanaka, T.; Matsuo, S.; Funabiki, T.; Yoshida, S. *J. Chem. Soc., Chem. Commun.* **1995**, 761.
(35) Yoshida, H.; Kimura, K.; Inaki, Y.; Hattori, T. *Chem. Commun.* **1997**, 129.
(36) Inaki, Y.; Yoshida, H.; Kimura, K.; Hattori, T. *J. Phys. Chem. B* **2000**, *104*, 10304.
(37) Inaki, Y.; Yoshida, H.; Kimura, K.; Inagaki, S.; Fukushima, Y.; Hattori, T. *Phys. Chem. Chem. Phys.* **2000**, *2*, 5293.
(38) Gao, X.; Wachs, I. E. *Catal. Today* **1999**, *51*, 233.
(39) Gao, X.; Bare, S. R.; Fierro, J. L. G.; Banares, M. A.; Wachs, I. E. *J. Phys. Chem. B* **1998**, *102*, 5653.
(40) Bordiga, S.; Colucia, S.; Lamberti, C.; Marchese, L.; Zecchina, A.; Boscherimi, F.; Buffa, F.; Genomi, F.; Leofanti, G.; Petrini, G.; Vlaic, G. *J. Phys. Chem.* **1994**, *98*, 4125.
(41) Howe, R. F.; Gratzel, M. *J. Phys. Chem.* **1985**, *89*, 4495.
(42) Mimic, O. I.; Zhang, Y.; Cromack, K. R.; Trifunic, A. D.; Thurnaur, M. C. *J. Phys. Chem.* **1993**, *97*, 7277.
(43) Mimic, O. I.; Zhang, Y.; Cromack, K. R.; Trifunic, A. D.; Thurnaur, M. C. *J. Phys. Chem.* **1993**, *97*, 13284.
(44) Rajh, T.; Ostafin, A. E.; Mimic, O. I.; Tiede, D. M.; Thurnaur, M. C. *J. Phys. Chem.* **1996**, *100*, 4538.
(45) Ahn, S. W.; Kevan, L. *J. Chem. Soc., Faraday Trans.* **1998**, *94*, 3147.
(46) Prakash, A. M.; Sung-Suh, H.; Kevan, L. *J. Phys. Chem. B* **1998**, *102*, 857.
(47) Abou-Kais, A.; Vedrine, J. C.; Masserdier, J. *J. Chem. Soc., Faraday Trans.* **1975**, *71*, 1697.
(48) Shiotani, M.; Moro, G.; Freed, J. H. *J. Chem. Phys.* **1981**, *74*, 2616.
(49) Anpo, M.; Aikawa, N.; Kubokawa, Y.; Che, M.; Louis, C.; Giamello, E. *J. Phys. Chem.* **1985**, *89*, 5689.
(50) Che, M.; Tench, A. J. *Adv. Catal.* **1983**, *32*, 1 and references therein.
(51) Nikisha, V. V.; Shelimov, B. N.; Kazansky, V. B. *Kinet. Katal.* **1974**, *15*, 676.
(52) Nikisha, V. V.; Shelimov, B. N.; Shvets, V. A.; Griva, A. P.; Kazansky, V. B. *J. Catal.* **1973**, *28*, 230.

(53) Shelimov, B. N.; Naccache, C.; Che, M. *J. Catal.* **1975**, *37*, 279.
(54) Iwamoto, M.; Lansford, J. H. *Chem. Phys. Lett.* **1979**, *66*, 48.
(55) Anpo, M.; Kubokawa, Y.; Fuji, T.; Suzuki, S. *J. Phys. Chem.* **1984**, *88*, 2572.
(56) Ogata, A.; Kazusaka, A.; Enyo, M. *J. Phys. Chem.* **1986**, *90*, 5201.
(57) Eigata, H.; Ogata, A.; Futamura, S.; Ibusuki, T. *Chem. Phys. Lett.* **2001**, *338*, 303.
(58) Fessenden, R. W.; Schuler, R. H. *J. Chem. Phys.* **1963**, *39*, 2147.
(59) Ichikawa, T.; Kagei, K.; Tachikawa, H.; Ishitani, Y. *J. Phys. Chem. A* **1999**, *103*, 6288.
(60) Okamoto, Y.; Imanaka, T.; Teranishi, S. *Bull. Chem. Soc. Jpn.* **1973**, *46*, 4.
(61) Kanai, H.; Shono, M.; Hamada, K.; Imamura, S. *J. Mol. Catal. A* **2001**, *172*, 25.
(62) Yoshida, S.; Tanaka, T.; Okada, M.; Funabiki, T. *J. Chem. Soc., Faraday Trans.* **1984**, *80*, 119.
(63) Moro-oka, Y.; Akita, M. *Catal. Today* **1998**, *41*, 327.
(64) Moro-oka, Y. *Catal. Today* **1998**, *45*, 3.
(65) Hoenett, B. K. *Heterogeneous Catalytic Oxidation*; John Willey & Sons, Ltd: Chichester, U.K., 2000; pp 161−188.
(66) Sheldon, R. A.; Bekkum, H. *Fine Chemicals through Heterogeneous Catalysis*; Wiley-VCH: Weinheim, 2001; pp 473−490.
(67) Sheldon, R. *Aspects of Homogeneous Catalysis*; Reidel: Weinheim, 1981; Vol. 4, pp 3−70.
(68) Wallar, B. J.; Lipscomb, J. D. *Chem. Rev.* **1996**, *96*, 2625.
(69) Tanaka, K. *J. Phys. Chem.* **1974**, *78*, 555.
(70) Tanaka, K.; Miyahara, K. *J. Phys. Chem.* **1974**, *78*, 2303.
(71) Courbon, H.; Formenti, M.; Pichat, P. *J. Phys. Chem.* **1977**, *81*, 550.
(72) Takita, Y.; Iwamoto, M.; Lansford, J. H. *J. Phys. Chem.* **1980**, *84*, 1710.
(73) Kubokawa, Y.; Anpo, M.; Yun, C. *Proceeding of the 7th international congress on catalysis*; Elsevier: 1980; p 1170.